Fra1 is required for TGFβ1 induced collective invasion

Sharon Camacho#, Apsra Nasir#, Raneen Rahhal, Maia Dominguez

and Gray W. Pearson*

Lombardi Comprehensive Cancer Center and Department of Oncology,

Georgetown University, Washington, DC 20057.

# Equal contribution

* To whom correspondence should be addressed.

Gray W. Pearson

Lombardi Comprehensive Cancer Center

Georgetown University

3970 Reservoir Road NW,

Washington, DC 20057

Phone- 202-687-0607

E-mail: **gp507@georgetown.edu**

Running title: Fra1 dictates the mode of tumor invasion

The authors declare no potential conflicts of interest.

ABSTRACT

Cells that lead collective invasion can have distinct traits and regulatory programs compared to the cells that follow them. Notably, a specific type of epithelial-to-mesenchymal transition (EMT) program we term a “trailblazer EMT” endows cells with the ability to lead collective invasion and promote the opportunistic invasion of intrinsically less invasive siblings. Here, we sought to define the regulatory programs that are responsible for inducing a trailblazer EMT in a genetically engineered mouse (GEM) model of breast cancer. Analysis of fresh tumor explants, cultured organoids and cell lines revealed that the trailblazer EMT was controlled by TGFβ pathway activity that induced a hybrid EMT state characterized by cells expressing E-cadherin and Vimentin. Notably, the trailblazer EMT was active in cells lacking keratin 14 expression and evidence of trailblazer EMT activation was detected in collectively invading cells in primary tumors. The trailblazer EMT program required expression of the transcription factor Fra1, which was regulated by the parallel autocrine activation of the epidermal growth factor receptor (EGFR) and extracellular signal regulated kinases (ERK) 1 and 2. Together, these results reveal that the activity of parallel TGFβ and EGFR pathways confers cells with the ability to lead collective invasion through the induction of a trailblazer EMT.

INTRODUCTION

Epithelial-to-mesenchymal transition (EMT) program activation is an established feature of primary tumors that promotes tumor progression and metastasis (1). Rather than being a single program, there are a wide range of EMTs that are regulated by diverse activation mechanisms and have unique molecular properties (2,3). This variability allows specific EMT programs to confer distinct functional traits, including invasive behavior (4), tumor initiating activity (5), suppression of the immune system (6) and resistance to therapeutics (7). Different EMT programs can be active in tumor subpopulations (4,8), raising the potential for complementary functions of cells in distinct EMT states. Indeed, specific types of EMT programs that influence tumor population properties have begun to be discovered (9). Notably, there are EMTs in which cells are endowed with the ability to influence the invasive behavior of non-EMT induced siblings (10,11). A "trailblazer EMT" program confers cells with an enhanced ability to initiate the collective invasion of adherent multicellular units through the extracellular matrix (ECM) (12). Collective invasion is the most frequent type of invasion detected in primary tumors (13-15). Collective invasion may also contribute to the dissemination of tumor clusters that seed metastases (16,17). Thus, understanding trailblazer EMTs is necessary to understand a common mode of local dissemination and a potential mode of metastasis.

During collective invasion, leading tumor cells extend actin-rich protrusions that deliver proteases and exert physical forces to reorganize the surrounding ECM into parallel fibrils (18,19). The lead cell then migrates along the newly created microtracks into the ECM. Additional cells subsequently invade by following the microtracks created by the lead cell (20). A trailblazer EMT confers cells with an enhanced ability to promote the formation of microtracks (12,21). Notably, cells that promote microtack generation induce the collective invasion of "opportunist" siblings that have not undergone a trailblazer EMT and have a relatively diminished intrinsic invasive ability (12,22,23). The interaction between trailblazer and opportunist cells can promote the progression from ductal carcinoma in situ (DCIS) to invasive breast

cancer (IBC) in an orthotopic tumor model (21). Consistent with results obtained with these experimental models, the interaction of distinct subpopulations is observed during the initial transition from DCIS to IBC in breast cancer patients (24,25). Trailblazer cells are also capable of metastasizing to the lung (12). Signaling programs that are specifically required for trailblazer cells to initiate collective invasion are required for metastasis and their expression correlates with poor breast cancer patient outcome (12,26), underscoring the critical function of trailblazer subpopulations during tumor progression.

The trailblazer EMT program includes genes that are specifically required for cells to initiate collective invasion, but are dispensable for other types of cell movement, including migration along two-dimensional surfaces (12,26). One of these trailblazer EMT genes is the guanine nucleotide exchange factor (GEF) DOCK10, which activates Cdc42 and N-Wasp to promote actin polymerization and protrusion formation. Others include PDGFRA, VASN and ITGA11 (12). Thus, the functional programs that directly contribute to the unique properties of a trailblazer EMT have begun to be defined. By comparison, the signaling programs that initiate a trailblazer EMT are poorly understood. To address this question we defined factors that promote a trailblazer EMT in the C3TAg genetically engineered mouse model of breast cancer (27). The tumors that develop in this model are molecularly similar to basal type breast cancer, which is frequently classified as triple-negative (no estrogen receptor, progesterone receptor or HER2 expression) (28,29). Through analysis of protein expression in primary tumors and functional testing in freshly derived tumor organoids, cultured organoids and primary cell lines we discovered that TGFβ induces a trailblazer EMT in hybrid cells with canonical mesenchymal and epithelial traits. Importantly, expression of the transcription factor Fra1 is necessary for this trailblazer EMT. Fra1 is not regulated by TGFβ pathway activity. Instead, the autocrine activation of EGFR and ERK1/2 is sufficient to promote Fra1 expression and permit a trailblazer EMT. Together, these results reveal that the integration of parallel signaling pathways coordinates the induction of a trailblazer EMT.

METHODS

Cell Culture. Cells were generated from C3TAg tumors as indicated, cultured as described (12,30) and verified by Powerplex genotyping. Cells were tested for mycoplasma (Lonza, LT07-703) prior the creation of freezedown stocks. Cells from these frozen stocks were routinely used within 25 passages. Tumor organoids were propagated in Organoid Media (DMEM/F12 (Corning, 10-092-CV), B27 (Fisher, 17504001), ITS (Lonza, 17-838Z), non-essential amino acids (Sigma, M7145), 10 ng/ml FGF2 (Peprotech, 100-18C) 50 ng/ml EGF (Peprotech, AF-100-15), Y27632 (Peprotech, 1293823) N-acetylcysteine (MP Biomedicals, 194603) and A83-01 (Peprotech, 9094360) **(Table S1)**. Organoids were passaged at least once per week by dissociating tumor organoids with Dispase (Sigma, SCM133) and TryPLE (Gibco, 12605-010) into single cell suspensions. The cell suspensions in plated at a density of 200,000-500,000 cells per well in a 24-well ultra low adhesion plate in Organoid Media. Virus was produced and cells were infected to generate stable cell lines as described (31).

3D culture experiments. Growth factor reduced Matrigel (Corning, 10-12 mg/ml stock concentration, #354230) and rat tail (Corning, #354236) collagen I were used for invasion assay experiments. Vertical invasion assays and experiments in 3D culture were performed and quantified as described previously using a Matrigel/Collagen I matrix (3-5 mg/ml Matrigel and 1.8-2.1 mg/ml Collagen I) (12,26). A 120 µm span on the z-axis is shown for the vertical invasion assays. For spheroid cluster experiments employing cell lines, 96-well Nunclon Sphera low adhesion plates (Thermo Scientific, 174925) were used to form clusters. 1000 cells per well were plated and incubated at 37˚C for 24-72 h. Clusters were then resuspended in 30 µl of Matrigel/Collagen I mix and plated on 20 µl of a basement layer of Matrigel/Collagen I and allowed to invade for 24 h. For 1339 organoid invasion assays, 200,000-500,000 cells were plated per well in a 24-well ultra low adhesion plate in Organoid Media. The cells were allowed to clump overnight. Clumps were then resuspended in 30 µl of Matrigel/Collagen I mix and plated on 20 µl of basement layer of Matrigel/Collagen I and allowed to invade for 24 h-48 h.

Immunoblot analysis, IF and IHC. Experiments and analysis were performed as described (12) using antibodies detailed in **Table S2.**

siRNA experiments. Cells were transfected with 50 nM of siRNA using RNAiMax transfection reagent (Invitrogen) for 48-72 h. The siRNAs were from Dharmacon and Sigma. Cells in all conditions designated as "Control" were transfected with a pool of siRNAs that does not target human genes. The details of the sequences and catalog numbers for each siRNA are located in **Table S3**.

Quantitative real-time PCR. Experiments were performed as described (12) using primer sequences listed in **Table S4**.

Mice. The C3-Tag [FVB-Tg(C3-1-TAg)cJeg/JegJ] mice (27) were a gift from Anna Riegel. Mice were housed and bred in accordance with a protocol approved by the Institutional Animal Use and Care Committee at Georgetown University in compliance with the NIH Guide for the Care and Use of Laboratory animals. Female mice were used for all analyses.

Tumor explants. The largest tumors from female C3TAg mice were minced and tumors were digested for up to 120 min at 37°C in a mixture of 1mg/ml Collagenase, 2U/µl DNase, 5% FBS in DMEM/F12. Digested tumors were pelleted at 80 x g for 1 min and the supernatant was discarded. Tumor organoids were then rinsed up to 5 times in 10 ml 5% FBS in DMEM/F12. Organoids were plated in a mixture of 30 ul of 2.4 mg/ml Rat tail collagen (354236, Corning) and 3 mg/ml growth factor reduced Matrigel onto a base layer of 20 µl of Collagen I/Matrigel. The organoids in ECM were overlaid with DMEM/F12 supplemented with

1% FBS, 1X ITS (Sigma, I3146), non-essential amino acids (Sigma, M7145) and 10 ng/ml FGF2 (Peprotech, 100-18C). Organoids were allowed to invade for 48 h, fixed and imaged unless otherwise indicated (12).

Statistical Methods. Data with a normal distribution determined by Shapiro-Wilk test were analyzed by two tailed Student's t-test (Graphpad Prism). Data that did not pass a normality test were analyzed by Mann-Whitney U test.

RESULTS

K14-high and K14-low C3Tag tumor cells lead collective invasion.

To understand how a trailblazer state is induced we investigated the invasive properties of C3TAg tumor organoids. Consistent with previous observations (21,32), there was heterogeneity in the invasive behavior of organoids derived from C3TAg tumors **(Fig. 1A)**. Intrinsic variability in invasive properties was also observed after tumors were dissociated into smaller cellular clusters (<5 cells) and allowed to grow in 3D culture for 4 days, with many actively growing organoids having less invasive character, indicating that diminished fitness was not the cause of reduced invasion **(Fig. 1A and S1A)**. Clonal populations of B6 and D6 cells derived from a C3TAg tumor also had distinct invasive properties **(Fig. S1B)**. Given this variability we next determined how cells with different intrinsic invasive properties interacted with each other. Interestingly, the noninvasive B6 cells were induced to opportunistically invade behind invasive cells from fresh C3TAg tumors, or the sibling invasive D6 clone **(Fig. 1B and S1B)**. This indicated that the invasive cells in C3TAg tumors and invasive clonal populations can function as trailblazer cells that lead the invasion of intrinsically less invasive opportunist siblings. Indeed, the noninvasive B6 clone expressed the transcription factor DNp63 **(Fig. S1C)**, which is detected in opportunist cells derived from human cell lines. DNp63 expressing cells also opportunistically invade in C3TAg tumors and C3TAg tumor explants (21).

The activation of a basal gene expression program exemplified by the expression of K14 correlates with invasion in the PyMT GEM model of luminal B type breast cancer (32). Invading cells in the C3TAg model express K14 **(Fig. 1C)**. However, we found that K14 expression alone did not correlate with trailblazer behavior in C3T organoids **(Fig. 1C)**. This was indicated by invasion being led by K8-high/K14-low cells in explants and primary tumors **(Fig. 1D)**. Moreover, depletion of K14 from 1863 cells derived from a C3TAg tumor only modestly reduced the extent of invasion, indicating that high K14 expression is not essential for C3TAg trailblazer cells to lead collective invasion **(Fig. 1E)**. Thus, our data indicated that

additional signaling programs beyond the control of K14 expression conferred a trailblazer EMT in C3TAg tumor cells.

A TGFβ1 induced hybrid EMT confers C3Tag cells with the ability to lead invasion.

To test how EMT state influenced the invasive properties of C3Tag tumor cells, we determined how TGFβ1, a canonical inducer of EMT (9), influenced the invasive behavior the 1339 organoid line derived from a C3Tag tumor **(Fig. 2A)**. Soluble TGFβ1 enhanced the extent of collective invasion of 1339 organoids within 48 h of treatment **(Fig. 2A)**. In addition, tumors that develop from 1339 organoids after orthotopic injection were more invasive than the 1339 organoid line itself, consistent with TGFβ1 in the microenvironment inducing a trailblazer EMT in vivo **(Fig. S2A)**. Inhibitors of a receptor for TGFβ1, TGFBR1, blocked the TGFβ1 induced trailblazer EMT in 1339 organoids **(Fig. 2A)**. A cell line (1863) also retained epithelial properties when established with a TGFBR1 inhibitor in the culture media, whereas cells derived from the same tumor (1863T) lost E-cadherin expression and displayed increased Vimentin expression, further indicated the ability of TGFβ1 to induce a trailblazer EMT **(Fig. S2B)**. A similar adoption of canonical mesenchymal features was observed in the trailblazer D6 clone that was also derived in the absence of a TGFBR1 inhibitor **(Fig. S2C)**. Brief exposure of 1 h to TGFβ1 is sufficient to confer a stable EMT state through a switch to a Ecadherin-low/Vimentin high state and makes cells independent of TGBFR activity (33). However, TGBFR1 inhibition suppressed the basal invasion of 1339 organoids and the invasion of C3TAg tumor explants, showing that TGBFR1 activity is required to sustain a trailblazer state **(Fig. 2A and B)**. These results indicated that trailblazer state in C3TAg tumor populations did not require a stable switch to fully mesenchymal state or independence from TGFBR1 activity. TGFβ1 induces gene expression changes through promoting the TGBFR1 dependent phosphorylation of the transcription factors SMAD2 and SMAD3 (34). The TGFβ1 induced invasion of 1863 cells required SMAD3 expression, indicating that TGFβ1 regulated gene expression program contributed to the observed trailblazer EMT **(Fig. 2C and S2D)**. SMAD3 depletion also reduced the invasion of mesenchymal 1863T cells, with similar re-

sults observed using 2 distinct siRNAs, showing that these cells also retained a requirement for TGFβ1 pathway activity **(Fig. S2E and F)**. Vimentin mRNA expression in 1339 organoids was increased within 48 h of TGFβ1 treatment, indicating that there was mesenchymal expression program activation **(Fig. 2D)**. However, cells retained E-cadherin expression and canonical EMT-TF expression was unchanged **(Fig. 2D)**. These results indicated that invading cells were in a hybrid EMT state. Analysis of C3T primary tumors showed that Vimentin expressing cells leading invasion at the tumor stromal boundary, indicating that EMT activation can occurs in collectively invading cells in the C3T primary tumors **(Fig. 2E)**.

Fra1 and ZEB1/2 expression promote a trailblazer EMT state.

To understand factors that control trailblazer EMT programs we next determined how canonical EMT regulatory factors influenced invasion in C3TAg tumors. TGFβ1 induced EMTs can involve suppression of miR200 family miRNAs (33). Indeed, transfection of 1863 and 1863T cells dramatically suppressed the invasion of spheroids and vertical invasion into the ECM from a cell monolayer **(Fig. 3A and S3A and B)**. miR200 suppresses ZEB1/2 expression in 1863T cells **(Fig. 3B)**, consistent with previous results in other models (35). Thus we further tested the potential function for ZEB1 and ZEB2 transcription factors in regulating the trailblazer state in cells derived from C3Tag tumors. Indeed, the combined depletion of both ZEB1/2 reduced 1863 spheroid invasion, consistent with the diminished invasion detected in cells in which ZEB1/2 are suppressed by exogenous miR200 **(Fig. 3C and 3D)**. By comparison, siRNAs targeting other canonical EMT TFs did not alter invasive behavior **(FIg. S3C)**. TGFβ1 signaling is integrated with other signaling networks, including programs that are regulated by AP-1 family transcription factors, which collaborate to regulate ZEB1/2 expression. Depletion of Fra1 reduced the TGFβ1 induced the invasion of 1863 spheroids **(Fig. 3E and F)**. Four distinct individual siRNAs and a second siRNA pool targeting Fra1 and a also suppressed the vertical invasion of 1863T cells **(Fig. 3F, S3D and E)**. Fra1 depletion reduced the invasion of D6 cells as well **(Fig. S3F)**. Fra1 interacts with c-Jun to regulate gene expression as an AP-1 complex (36). Indeed, c-Jun was required for the invasion of 1863T cells **(Fig. S3G)**, sug-

gesting Fra1 containing AP-1 complexes regulate the expression of genes necessary for trailblazer invasion. However, depletion of Fra1 did not alter ZEB1/2 expression, indicating that Fra1 regulated the trailblazer EMT state in independent of controlling ZEB1/2 expression in these cells **(Fig. 3G)**. Interestingly, Fra1 expression in 1339 organoids was not regulated by acute TGFβ1 stimulation and and was not dependent on TGFBR1 activity **(Fig. 3H and I)**. This indicated that the induction of Fra1 by a parallel signaling pathway is necessary for TGFβ1 to induce a trailblazer EMT state.

EGFR and ERK1/2 activity are necessary for Fra1 expression and the induction of trailblazer EMT.

We next determined how Fra1 expression was regulated in C3Tag tumor cells. ERK1/2 can promote Fra1 transcription and phosphorylation dependent stabilization (37). Treatment with trametinib, an inhibitor of MEK1/2, the upstream activators of ERK1/2, reduced Fra1 expression in 1863 cells **(Fig. 4A)**. Inhibition of MEK1/2 did not alter the phosphorylation of SMAD2 or ZEB1 expression, showing that ERK1/2 specifically regulates Fra1 expression. Consistent with these results, MEK1/2 inhibition with trametinib reduced TGFβ1 induced invasion of 1339 organoids **(Fig. 4B)**. Notably, the clinically approved MEK1/2 inhibitor Trametinib inhibited the invasion of explants derived from 4 different tumors **(Fig. 4C)**. Consistent with a requirement of ERK1/2 for invasion, active phosphorylated ERK1/2 was detected in collectively invading cells in C3TAg primary tumors **(Fig. 4D)**. ERK1/2 activity is cyclical in response to the activation of negative feedback loops (38). Thus, persistent ERK1/2 phosphorylation is not necessarily expected in all collectively invading cells. HER2 amplification can activate ERK1/2 and synergize with TGFβ1 signaling to promote invasion (39). However, C3TAg tumors do not have amplified HER2 expression (28). Autocrine activation of growth factor receptors can promote ERK1/2 phosphorylation (40). Indeed, the EGFR inhibitor Erlotinib suppressed Fra1 expression **(Fig. 4E)**. Erlotinib also suppressed the TGFβ1 induced invasion of 1339 organoids, indicating that autocrine EGFR activity and promoted the Fra1 expression that was necessary for invasion **(Fig. 4F)**.

DISCUSSION

Through investigating the requirements for invasion in primary tumor cells, we have revealed the molecular underpinnings of a hybrid EMT program that confers tumor cells with the ability to initiate collective invasion. It is well established that EMT programs confer tumor cells with invasive properties (41). One of the defining attributes of EMTs is the loss of epithelial character (42). This shift from an epithelial phenotype includes the reduced expression of certain cell-cell adhesion proteins (43). The loss of cell-cell cohesion facilitates the detachment of single cells, which can migrate through the ECM utilizing proteolytic and force dependent mechanisms (44). While conceptually straightforward, a model centered on the highly mesenchymal tumor populations invading as single cells does not account for the invasive properties of the majority of invasive populations in primary tumors (31). Tumor cells predominantly engage in multicellular collective invasion and retain epithelial traits, including E-cadherin expression. Indeed, E-cadherin expressing cells are fully capable of collective invasion (30,45). These observations have contributed to a revised understanding of EMTs as being variable in their molecular properties as opposed to a single program that ultimately leads to a fully mesenchymal state (46). This recognition of the existence of hybrid EMTs has created a new challenge of defining their function in tumors. Our results show that there is a hybrid trailblazer EMT state. Analysis of human cancer cell lines had shown a correlation with a full mesenchymal state (12,18). However, there was no indication that the loss of epithelial character was necessary for a trailblazer EMT. Thus, the specific attributes of trailblazer EMTs has remained unclear. Our results suggest that the unique properties of a trailblazer EMT that promote ECM reorganization can be acquired while cells retain epithelial character. Thus, our results support future investigations focused on regulatory processes that support features of collective invasion rather than only relying on canonical EMT markers to define the contribution of EMTs to invasive cell phenotypes.

The induction of a trailblazer EMT in the C3TAg model promoted the invasion of cells with low or undetectable levels of K14 expression. K14 expression is a hallmark of collectively invading cells in the

PyMT GEM model of breast cancer and K14 positive cells collectively invade in breast cancer patient tumors (32). Consistent with our observations here, we have found that K14 expression is not required for human trailblazer breast cancer cells to collectively invade (12). This suggests that the specific requirements for a trailblazer EMT may depend on cell intrinsic properties that vary between tumor type. We found that expression of the transcription factor Fra1 was necessary for a trailblazer EMT in cells derived from C3TAg tumors. In addition, inhibition of the autocrine signaling pathway that promotes Fra1 expression blunts the TGFβ1 induced trailblazer EMT in cultured C3TAg organoids and the invasion of fresh organoids from primary tumors. TGFβ1 signaling did not modulate Fra1 expression in C3TAg tumor cells. Thus, the control of Fra1 was a cell intrinsic property in the context in which we evaluated collective invasion. Whether Fra1 controls a regulatory program distinct from the program active in K14 expressing cells, and thus providing an alternative type of trailblazer EMT is an interesting line of future investigation.

In summary, we have found that the integration of TGFβ1 and EGFR-ERK1/2-Fra1 pathways is necessary for a trailblazer EMT program. Our results suggest that disruption of either pathway is sufficient to blunt the collective invasion of tumor organoids. Thus, our results suggest the potential use of existing therapeutic agents to limit breast cancer cell collective invasion.

ACKNOWLEDGEMENTS. Work was supported by NIH R01CA218670, Georgetown Women and Wine (G. Pearson), NIH T32CA009686 (S. Camacho) and NIH P30CA051008 for shared resources (G. Pearson).

REFERENCES

1. Chaffer CL, San Juan BP, Lim E, Weinberg RA. EMT, cell plasticity and metastasis. Cancer Metastasis Rev 2016;35:645-54.

2. Jolly MK, Ward C, Eapen MS, Myers S, Hallgren O, Levine H, et al. Epithelial-mesenchymal transition, a spectrum of states: Role in lung development, homeostasis, and disease. Dev Dyn 2018;247:346-58.

3. Pastushenko I, Blanpain C. EMT Transition States during Tumor Progression and Metastasis. Trends Cell Biol 2019;29:212-26.

4. Aiello NM, Maddipati R, Norgard RJ, Balli D, Li J, Yuan S, et al. EMT Subtype Influences Epithelial Plasticity and Mode of Cell Migration. Dev Cell 2018;45:681-95 e4.

5. Mani SA, Guo W, Liao MJ, Eaton EN, Ayyanan A, Zhou AY, et al. The epithelial-mesenchymal transition generates cells with properties of stem cells. Cell 2008;133:704-15.

6. Terry S, Savagner P, Ortiz-Cuaran S, Mahjoubi L, Saintigny P, Thiery JP, et al. New insights into the role of EMT in tumor immune escape. Mol Oncol 2017;11:824-46.

7. Singh A, Settleman J. EMT, cancer stem cells and drug resistance: an emerging axis of evil in the war on cancer. Oncogene 2010;29:4741-51.

8. Pastushenko I, Brisebarre A, Sifrim A, Fioramonti M, Revenco T, Boumahdi S, et al. Identification of the tumour transition states occurring during EMT. Nature 2018;556:463-68.

9. Pearson GW. Control of Invasion by Epithelial-to-Mesenchymal Transition Programs during Metastasis. Journal of clinical medicine 2019;8.

10. Celia-Terrassa T, Meca-Cortes O, Mateo F, de Paz AM, Rubio N, Arnal-Estape A, et al. Epithelial-mesenchymal transition can suppress major attributes of human epithelial tumor-initiating cells. J Clin Invest 2012;122:1849-68.

11. Neelakantan D, Zhou H, Oliphant MUJ, Zhang X, Simon LM, Henke DM, et al. EMT cells increase breast cancer metastasis via paracrine GLI activation in neighbouring tumour cells. Nature communications 2017;8:15773.

12. Westcott JM, Prechtl AM, Maine EA, Dang TT, Esparza MA, Sun H, et al. An epigenetically distinct breast cancer cell subpopulation promotes collective invasion. J Clin Invest 2015;125:1927-43.

13. Friedl P, Hegerfeldt Y, Tusch M. Collective cell migration in morphogenesis and cancer. Int J Dev Biol 2004;48:441-9.

14. Nguyen-Ngoc KV, Cheung KJ, Brenot A, Shamir ER, Gray RS, Hines WC, et al. ECM microenvironment regulates collective migration and local dissemination in normal and malignant mammary epithelium. Proc Natl Acad Sci U S A 2012;109:E2595-604.

15. Bronsert P, Enderle-Ammour K, Bader M, Timme S, Kuehs M, Csanadi A, et al. Cancer cell invasion and EMT marker expression: a three-dimensional study of the human cancer-host interface. J Pathol 2014;234:410-22.

16. Aceto N, Bardia A, Miyamoto DT, Donaldson MC, Wittner BS, Spencer JA, et al. Circulating tumor cell clusters are oligoclonal precursors of breast cancer metastasis. Cell 2014;158:1110-22.

17. Cheung KJ, Padmanaban V, Silvestri V, Schipper K, Cohen JD, Fairchild AN, et al. Polyclonal breast cancer metastases arise from collective dissemination of keratin 14-expressing tumor cell clusters. Proc Natl Acad Sci U S A 2016;113:E854-63.

18. Wolf K, Wu YI, Liu Y, Geiger J, Tam E, Overall C, et al. Multi-step pericellular proteolysis controls the transition from individual to collective cancer cell invasion. Nat Cell Biol 2007;9:893-904.

19. Yu X, Zech T, McDonald L, Gonzalez EG, Li A, Macpherson I, et al. N-WASP coordinates the delivery and F-actin-mediated capture of MT1-MMP at invasive pseudopods. J Cell Biol 2012;199:527-44.

20. Friedl P, Alexander S. Cancer invasion and the microenvironment: plasticity and reciprocity. Cell 2011;147:992-1009.

21. Westcott JM, Camacho S, Nasir A, Huysman ME, Rahhal R, Dang TT, et al. DeltaNp63 regulated epithelial-to-mesenchymal transition state heterogeneity confers a leader-follower relationship that drives collective invasion. Cancer Res 2020.

22. Kim YH, Choi YW, Lee J, Soh EY, Kim JH, Park TJ. Senescent tumor cells lead the collective invasion in thyroid cancer. Nature communications 2017;8:15208.

23. Konen J, Summerbell E, Dwivedi B, Galior K, Hou Y, Rusnak L, et al. Image-guided genomics of phenotypically heterogeneous populations reveals vascular signalling during symbiotic collective cancer invasion. Nature communications 2017;8:15078.

24. Park SY, Gonen M, Kim HJ, Michor F, Polyak K. Cellular and genetic diversity in the progression of in situ human breast carcinomas to an invasive phenotype. J Clin Invest 2010;120:636-44.

25. Casasent AK, Schalck A, Gao R, Sei E, Long A, Pangburn W, et al. Multiclonal Invasion in Breast Tumors Identified by Topographic Single Cell Sequencing. Cell 2018;172:205-17 e12.

26. Maine EA, Westcott JM, Prechtl AM, Dang TT, Whitehurst AW, Pearson GW. The cancer-testis antigens SPANX-A/C/D and CTAG2 promote breast cancer invasion. Oncotarget 2016;7:14708-26.

27. Green JE, Shibata MA, Yoshidome K, Liu ML, Jorcyk C, Anver MR, et al. The C3(1)/SV40 T-antigen transgenic mouse model of mammary cancer: ductal epithelial cell targeting with multistage progression to carcinoma. Oncogene 2000;19:1020-7.

28. Herschkowitz JI, Simin K, Weigman VJ, Mikaelian I, Usary J, Hu Z, et al. Identification of conserved gene expression features between murine mammary carcinoma models and human breast tumors. Genome Biol 2007;8:R76.

29. Cheang MC, Voduc D, Bajdik C, Leung S, McKinney S, Chia SK, et al. Basal-like breast cancer defined by five biomarkers has superior prognostic value than triple-negative phenotype. Clin Cancer Res 2008;14:1368-76.

30. Dang TT, Esparza MA, Maine EA, Westcott JM, Pearson GW. DeltaNp63alpha Promotes Breast Cancer Cell Motility through the Selective Activation of Components of the Epithelial-to-Mesenchymal Transition Program. Cancer Res 2015;75:3925-35.

31. Dang TT, Prechtl AM, Pearson GW. Breast cancer subtype-specific interactions with the microenvironment dictate mechanisms of invasion. Cancer Res 2011;71:6857-66.

32. Cheung KJ, Gabrielson E, Werb Z, Ewald AJ. Collective invasion in breast cancer requires a conserved basal epithelial program. Cell 2013;155:1639-51.

33. Celia-Terrassa T, Bastian C, Liu DD, Ell B, Aiello NM, Wei Y, et al. Hysteresis control of epithelial-mesenchymal transition dynamics conveys a distinct program with enhanced metastatic ability. Nature communications 2018;9:5005.

34. Weiss A, Attisano L. The TGFbeta superfamily signaling pathway. Wiley interdisciplinary reviews Developmental biology 2013;2:47-63.

35. Gregory PA, Bert AG, Paterson EL, Barry SC, Tsykin A, Farshid G, et al. The miR-200 family and miR-205 regulate epithelial to mesenchymal transition by targeting ZEB1 and SIP1. Nat Cell Biol 2008;10:593-601.

36. Doehn U, Hauge C, Frank SR, Jensen CJ, Duda K, Nielsen JV, et al. RSK is a principal effector of the RAS-ERK pathway for eliciting a coordinate promotile/invasive gene program and phenotype in epithelial cells. Mol Cell 2009;35:511-22.

37. Pearson G, Robinson F, Beers Gibson T, Xu BE, Karandikar M, Berman K, et al. Mitogen-activated protein (MAP) kinase pathways: regulation and physiological functions. Endocr Rev 2001;22:153-83.

38. English J, Pearson G, Wilsbacher J, Swantek J, Karandikar M, Xu S, et al. New insights into the control of MAP kinase pathways. Exp Cell Res 1999;253:255-70.

39. Seton-Rogers SE, Lu Y, Hines LM, Koundinya M, LaBaer J, Muthuswamy SK, et al. Cooperation of the ErbB2 receptor and transforming growth factor beta in induction of migration and invasion in mammary epithelial cells. Proc Natl Acad Sci U S A 2004;101:1257-62.

40. Chen Z, Gibson TB, Robinson F, Silvestro L, Pearson G, Xu B, et al. MAP kinases. Chem Rev 2001;101:2449-76.

41. De Craene B, Berx G. Regulatory networks defining EMT during cancer initiation and progression. Nat Rev Cancer 2013;13:97-110.

42. Kalluri R, Weinberg RA. The basics of epithelial-mesenchymal transition. J Clin Invest 2009;119:1420-8.

43. Maeda M, Johnson KR, Wheelock MJ. Cadherin switching: essential for behavioral but not morphological changes during an epithelium-to-mesenchyme transition. J Cell Sci 2005;118:873-87.

44. Friedl P, Wolf K. Plasticity of cell migration: a multiscale tuning model. J Exp Med;207:11-9.

45. Shamir ER, Coutinho K, Georgess D, Auer M, Ewald AJ. Twist1-positive epithelial cells retain adhesive and proliferative capacity throughout dissemination. Biology open 2016;5:1216-28.

46. Jolly MK, Tripathi SC, Jia D, Mooney SM, Celiktas M, Hanash SM, et al. Stability of the hybrid epithelial/mesenchymal phenotype. Oncotarget 2016;7:27067-84.

FIGURE LEGENDS

Figure 1. K14-high and K14-low cells lead collective invasion. **A)** Model depicting tumor processing and analysis of organoids. Representative images show C3TAg organoids 24 h after embedding in ECM. Dissociated cells were analyzed after 4 days of growth. Violin plot shows quantification of circularity (Mann Whitney test, n=2 tumors). **B)** Representative images of multicellular clusters of the C3TAg-derived non-invasive B6 clone (H2B:mCherry) and C3TAg cells from fresh tumors. Cells were clustered in low adhesion wells alone or at a 1:1 ratio prior to embedding in ECM (n=3 tumors). **C)** K14 (magenta) and K8 (cyan) expression in C3TAg organoids. Graph shows quantification of keratin expression in the leading invasive cells (mean±SEM, n=3 tumors, unpaired Student's t test). **D)** K14 (magenta) and K8 (cyan) expression in C3TAg primary tumors. **E)** Invasion of 1863 spheroids after K14 and K8 depletion. Graph shows area of invading nuclei indicated by the image mask (mean±SEM, n=2, unpaired Student's t test). Scale bars, 50 µm.

Figure 2. A TGFβ1 induced hybrid EMT confers C3TAg cells with the ability to lead invasion. A) Workflow of the development of organoid lines from C3TAg tumors. The TGFBR1 inhibitors A83-01 (500 nM) and SB43152 (1 uM) suppress both intrinsic and TGFβ1 induced invasion of organoid lines. Violin plot shows quantification of circularity (Mann Whitney test, n=2 for SB43152, n>4 for A83-01). **B)** Model showing C3TAg tumor processing and treatment. Representative images show that A83-01 reduces the invasion of C3TAg organoids. Violin plot shows area of invading nuclei (Mann Whitney test, n=3 tumors). **C)** SMAD3 depletion suppresses the invasion of 1863 spheroids (mean±SEM, n=2, unpaired Student's t test). **D)** qPCR results showing that TGFβ1 (2ng/mL) treatment for 48 hrs induces Vimentin while expression of additional canonical EMT markers was unaltered (mean±SD, n=2). **E)** Vimetin expression (magenta) in C3TAg primary tumor cells indicated by SV40 (cyan) and K8 (white) expression. Scale bars, 50 µm.

Figure 3. Fra1 and ZEB1/2 expression promotes a trailblazer EMT state. A) Transfection of a miR200c-3p mimic decreases invasion of 1863 spheroids (mean±SD, n=2, unpaired Student's t test). **B)** qPCR showing that miR200c-3p suppresses Zeb1 and Zeb2 mRNA expression (mean±SEM, n=2). **C)** Simultaneous depletion of Zeb1 and Zeb2 reduces the invasion of 1863 spheroids (mean±SEM, n=3). **D)** qPCR showing the depletion of Zeb1 and Zeb2 after siRNA transfection (mean±SEM, n=2). **E)** Fra1 depletion decreases TGFβ1 induced invasion of 1863 spheroids. Graphs shows the area of invading nuclei (mean±SEM, n=5, unpaired Student's t test). **F)** Fra1 mRNA is depleted by two separate Fosl1 siRNA pools (mean±SEM, n=3 for pool 1 and n=2 for pool 2). **G)** qPCR showing that Fra1 depletion does not reduce Zeb1 and Zeb2 expression (mean±SD, n=2). **H)** qPCR showing that TGFβ1 treatment (2ng/mL for 48 hrs) does not increase Fra1 expression in 1339 organoids (mean±SD, n=2). **I)** qPCR showing that the TGFBR1 inhibitor A83-01 does not reduce Fra1 expression (mean±SD, n=2). Scale bars, 50 µm.

Figure 4. EGFR and ERK1/2 activity are necessary for Fra1 expression and the induction of a trailblazer EMT. A) Upper immunoblot shows Fra1 and phosphorylated Fra1 expression in 1863 cells treated with 50 nM of the MEK1/2 inhibitor Trametinib. ERK1/2 phosphorylation is reduced upon treatment. Lower immunoblot shows that Trametinib treatment does not reduce Zeb1 expression or SMAD2 phosphorylation (n=2). **B)** Representative images showing that Trametinib (50 nM) treatment suppresses the TGFβ1 induced invasion of 1339 organoids. Violin plot shows circularity quantification (Mann Whitney test, n=4). **C)** Representative images showing that Trametinib (50 nM) treatment suppresses the invasion of fresh C3Tag tumor organoids. Violin plot shows quantification of area of invading nuclei (Mann Whitney test, n=4 mice). **D)** Phosphorylated ERK1/2 (magenta) in C3TAg primary tumor cells indicated by SV40 (cyan) and K8 (white) expression. Scale bars, 50 µm. **E)** qPCR showing that inhibition of EGFR (Erlotinib) and ERK1/2 activity (Trametinib) suppresses Fra1 expression (mean±SD, n=2). **F)** Treatment with the EGFR inhibitor Erlotinib (1 uM) reduces TGFβ1 induced invasion of 1339 organoids. Violin plot shows circularity quantification (Mann Whitney test, n=4). Scale bars, 50 µm.

Figure 1

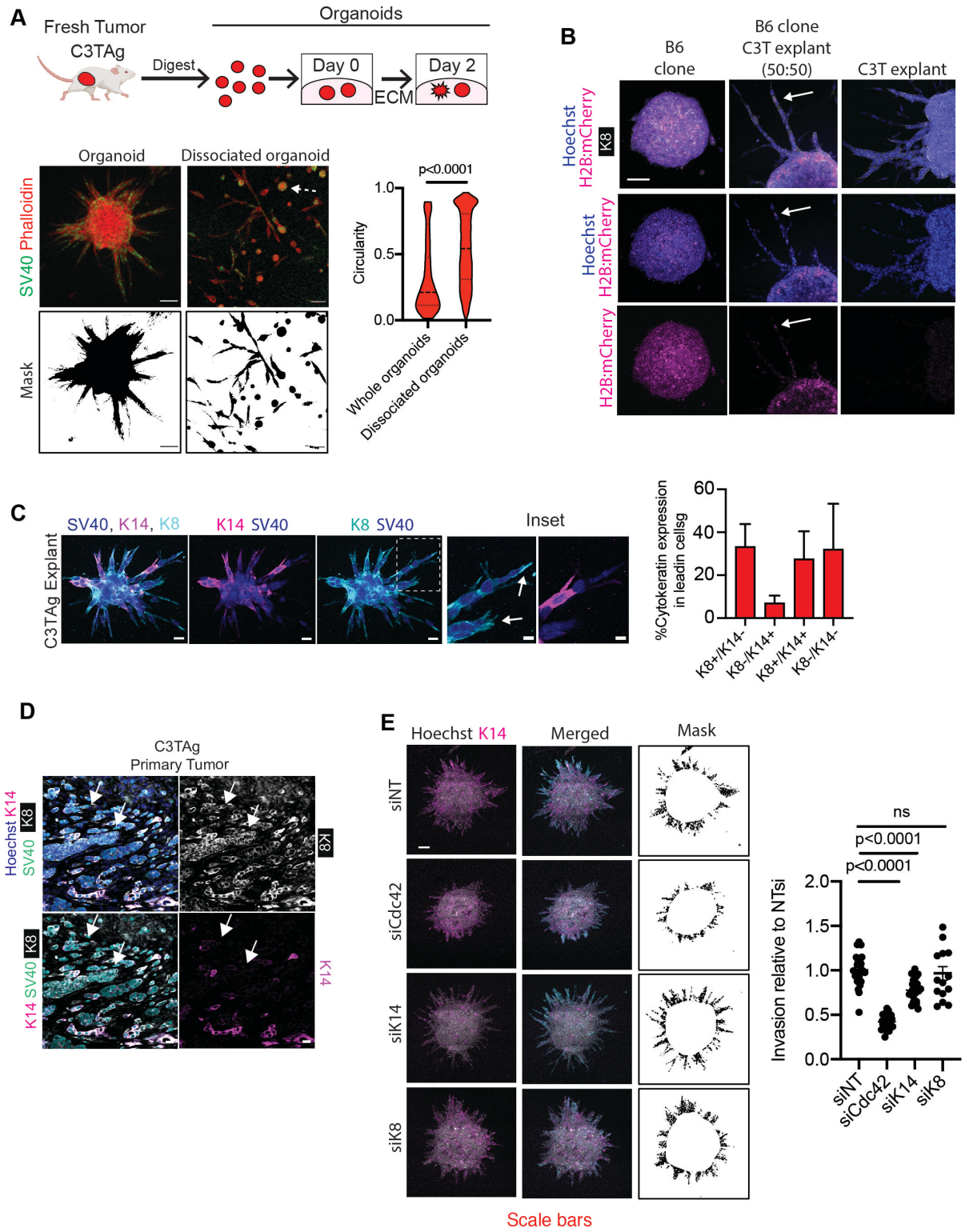
A
Fresh Tumor
C3TAg
Digest
Organoids
Day 0
Day 2
ECM
Organoid
Dissociated organoid
SV40 Phalloidin
Mask
p<0.0001
Circularity
1.0
0.5
0.0
Whole organoids
Dissociated organoids
B
B6 clone
B6 clone
C3T explant
(50:50)
C3T explant
Hoechst
H2B:mCherry
K8
H2B:mCherry
C
SV40, K14, K8
K14 SV40
K8 SV40
Inset
C3TAg Explant
%Cytokeratin expression
in leadin cellsg
60
40
20
0
K8+/K14-
K8-/K14+
K8+/K14+
K8-/K14-
D
C3TAg
Primary Tumor
Hoechst K14
SV40
K8
K14 SV40
K14
E
Hoechst K14
Merged
Mask
siNT
siCdc42
siK14
siK8
ns
p<0.0001
p<0.0001
Invasion relative to NTsi
2.0
1.5
1.0
0.5
0.0
siNT
siCdc42
siK14
siK8
Scale bars

Figure 2

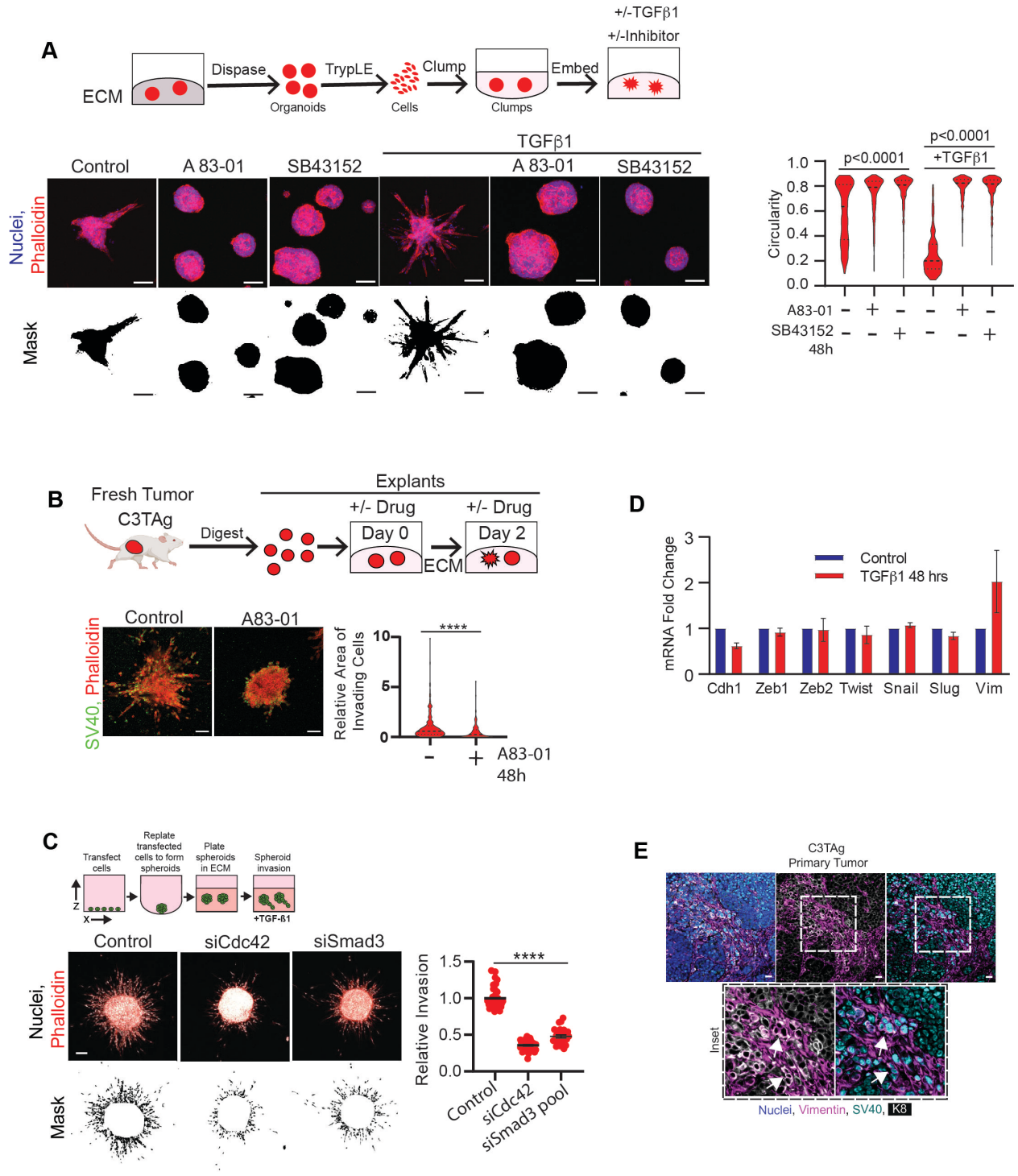
A
ECM
Dispase
Organoids
TrypLE
Cells
Clump
Clumps
Embed
+/-TGFβ1
+/-Inhibitor
Control
A 83-01
SB43152
TGFβ1
A 83-01
SB43152
Nuclei, Phalloidin
Mask
p<0.0001
p<0.0001
+TGFβ1
Circularity
1.0
0.8
0.6
0.4
0.2
0.0
A83-01 – + – – + –
SB43152 – – + – – +
48h
B
Fresh Tumor
C3TAg
Digest
Explants
+/- Drug
Day 0
+/- Drug
Day 2
ECM
Control
A83-01
SV40, Phalloidin
Relative Area of Invading Cells
10
5
0
****
– +
A83-01
48h
D
mRNA Fold Change
3
2
1
0
Control
TGFβ1 48 hrs
Cdh1
Zeb1
Zeb2
Twist
Snail
Slug
Vim
C
Transfect cells
Replate transfected cells to form spheroids
Plate spheroids in ECM
Spheroid invasion
+TGF-ß1
Control
siCdc42
siSmad3
Nuclei, Phalloidin
Mask
Relative Invasion
1.5
1.0
0.5
0.0
****
Control
siCdc42
siSmad3 pool
E
C3TAg
Primary Tumor
Inset
Nuclei, Vimentin, SV40, K8

Figure 3

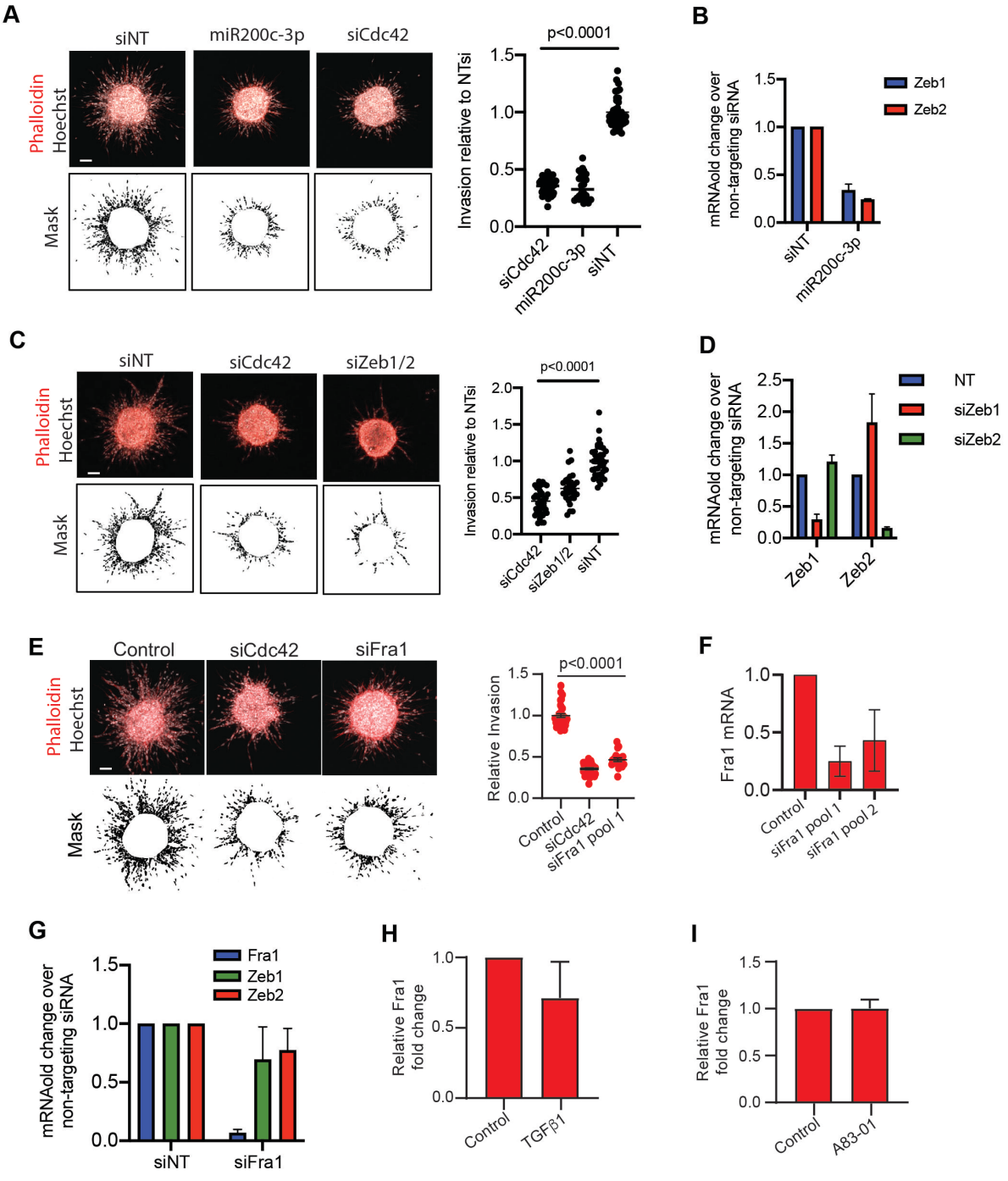
A
siNT
miR200c-3p
siCdc42
Phalloidin
Hoechst
Mask
p<0.0001
Invasion relative to NTsi
1.5
1.0
0.5
0.0
siCdc42
miR200c-3p
siNT
B
mRNAold change over non-targeting siRNA
Zeb1
Zeb2
siNT
miR200c-3p
C
siNT
siCdc42
siZeb1/2
Phalloidin
Hoechst
Mask
p<0.0001
Invasion relative to NTsi
2.0
siCdc42
siZeb1/2
siNT
D
mRNAold change over non-targeting siRNA
2.5
NT
siZeb1
siZeb2
Zeb1
Zeb2
E
Control
siCdc42
siFra1
Phalloidin
Hoechst
Mask
p<0.0001
Relative Invasion
Control
siCdc42
siFra1 pool 1
F
Fra1 mRNA
Control
siFra1 pool 1
siFra1 pool 2
G
mRNAold change over non-targeting siRNA
Fra1
Zeb1
Zeb2
siNT
siFra1
H
Relative Fra1 fold change
Control
TGFβ1
I
Relative Fra1 fold change
Control
A83-01

Figure 4

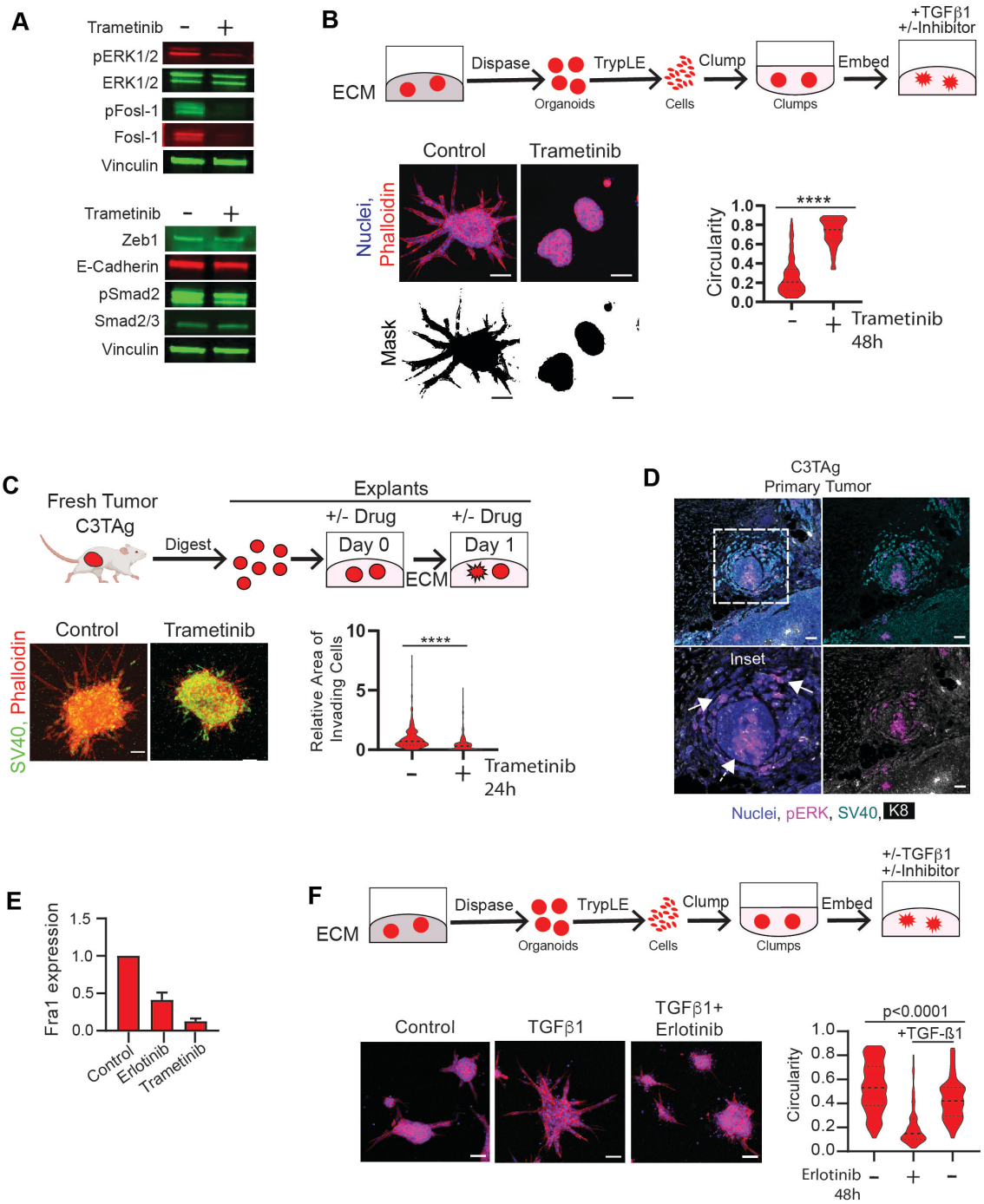
A
Trametinib - +
pERK1/2
ERK1/2
pFosl-1
Fosl-1
Vinculin
Trametinib - +
Zeb1
E-Cadherin
pSmad2
Smad2/3
Vinculin
B
ECM
Dispase
Organoids
TrypLE
Cells
Clump
Clumps
Embed
+TGFβ1
+/-Inhibitor
Control
Trametinib
Nuclei, Phalloidin
Mask
Circularity
****
Trametinib 48h
C
Fresh Tumor C3TAg
Digest
Explants
+/- Drug
Day 0
+/- Drug
Day 1
ECM
Control
Trametinib
SV40, Phalloidin
Relative Area of Invading Cells
****
Trametinib 24h
D
C3TAg Primary Tumor
Inset
Nuclei, pERK, SV40, K8
E
Fra1 expression
Control
Erlotinib
Trametinib
F
ECM
Dispase
Organoids
TrypLE
Cells
Clump
Clumps
Embed
+/-TGFβ1
+/-Inhibitor
Control
TGFβ1
TGFβ1+ Erlotinib
p<0.0001
+TGF-ß1
Circularity
Erlotinib 48h